High Pressure Pyrolysis of Toluene. 1. Experiments and Modeling of Toluene Decomposition

R. Sivaramakrishnan,[†] **Robert S. Tranter,**[‡] **and K. Brezinsky*,**[†]

Department of Mechanical & Industrial Engineering, University of Illinois at Chicago, Chicago, Illinois 60607, and Chemistry Division, Argonne National Laboratory, Argonne, Illinois 60439

The pyrolysis of toluene, the simplest methyl-substituted aromatic molecule, has been studied behind reflected shock waves using a single pulse shock tube. Experiments were performed at nominal high pressures of 27 and 45 bar and spanning a wide temperature range from 1200 to 1900 K. A variety of stable species, ranging from small hydrocarbons to single ring aromatics (principal soot precursors such as phenylacetylene and indene) were sampled from the shock tube and analyzed using standard gas chromatographic techniques. A detailed chemical kinetic model with 262 reactions and 87 species was assembled to simulate the stable species profiles (specifically toluene, benzene and methane) from the current high-pressure pyrolysis data sets and shock tube−atomic resonance absorption spectrometry (ARAS) H atom profiles obtained from prior toluene pyrolysis experiments performed under similar high-temperature conditions and lower pressures from 1.5 to 8 bar. The primary steps in toluene pyrolysis represent the most sensitive and dominant reactions in the model. Consequently, in the absence of unambiguous direct experimental measurements, we have utilized recent high level theoretical estimates of the barrierless association rate coefficients for these primary reactions, $C_6H_5 + CH_3 \rightarrow C_6H_5CH_3$ (1a) and $C_6H_5CH_2 + H \rightarrow C_6H_5CH_3$ (1b) in the detailed chemical kinetic model. The available data sets can be successfully reconciled with revised values for $\Delta H_f^0{}_{298K}(C_6H_5CH_2) = 51.5 \pm 1.0$ kcal/mol and $\Delta H_f^0{}_{298K}(C_6H_5) = 78.6 \pm 1.0$ kcal/mol that translate to primary dissociation rate constants, reverse of 1a and 1b, represented by $k_{-1a,\infty} = (4.62 \times 10^{25})T^{-2.53}\exp[-104.5 \times 10^3/RT]$ s^{-1} and $k_{-1b,\infty} = (1.524 \times 10^{16})T^{-0.04}\exp[-93.5 \times 10^3/RT]$ s^{-1} (R in units of cal/(mol K)). These high-pressure limiting rate constants suggest high-temperature branching ratios for the primary steps that vary from 0.39 to 0.52 over the temperature range 1200−1800 K.
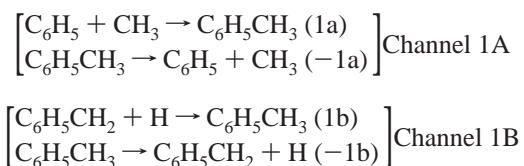
Introduction

The simplest methyl-substituted aromatic, toluene, occurs naturally in crude oils but is also formed during the refining of these oils and during the cracking of hydrocarbons to form light hydrocarbons such as ethylene and propylene. However because toluene is known to have a high energy density and antiknock rating, the majority of the toluene produced is not isolated from the refinery streams but is blended in with the gasoline pool. Currently toluene along with the xylenes forms the bulk of the aromatic content of a wide variety of commercial as well as premium and jet engine fuels (5−35% mole fraction in premium fuels). Because of its abundance, toluene has been suggested to be the surrogate single ring aromatic for gasoline, diesel, and aviation fuels in a recent CHEMKIN workshop[1] in line with the recommendations made in an earlier workshop on surrogate fuels.[2]

Despite the commercial and industrial significance of toluene there is very limited information on the detailed kinetics that govern its combustion and the subsequent secondary chemistry that is relevant to intermediates formation and is essential for emissions considerations. Furthermore, an important consideration to be taken note of from the viewpoint of combustion chemists is the fact that these primary aromatics such as toluene are the precursors for the formation of soot which not only decreases combustion efficiency but is also a major emissions concern. Recent studies[3] have also highlighted the toxic and carcinogenic effects of soot particles. To gain a better under-

standing of soot production (also useful for the production of products such as carbon black), the gas-phase chemistry involved in burning key soot precursor molecules such as toluene forms a vital and primary component.

Toluene pyrolysis studies have been initiated as early as in the 1940s with the seminal work by Szwarc[4,5] resulting in the estimation of the C−H bond energy in the substituted methyl group in toluene and its widespread usage as a radical scavenger. Szwarc's[4] experiments were confined to the intermediate temperature range from 1000 to 1170 K. The bulk of the experimental studies on toluene pyrolysis[6−14] after Szwarc's early experiments have been reviewed in the modeling studies by Kern et al.[15] and Lindstedt and Maurice.[16] The majority of the experimental studies[8−13] were initiated with the main objective being the estimation of the primary dissociation rate coefficients in toluene via reactions −1a and −1b. Kern et al.[15] modeled all the available high-temperature data on toluene pyrolysis and highlighted that both the initiation channels (1A and 1B) were important in contrast to prior recommendations[10,11,13] that the only important reaction at high temperatures was the C−H fission channel (1B). Lindstedt and Maurice[16]

$$\left[\begin{array}{l} C_6H_5 + CH_3 \rightarrow C_6H_5CH_3 \ (1a) \\ C_6H_5CH_3 \rightarrow C_6H_5 + CH_3 \ (-1a) \end{array}\right] \text{Channel 1A}$$

$$\left[\begin{array}{l} C_6H_5CH_2 + H \rightarrow C_6H_5CH_3 \ (1b) \\ C_6H_5CH_3 \rightarrow C_6H_5CH_2 + H \ (-1b) \end{array}\right] \text{Channel 1B}$$

developed a detailed chemical kinetic model to describe the high-temperature pyrolysis and oxidation of toluene.

* Corresponding author. E-mail: Kenbrez@uic.edu.
† University of Illinois at Chicago.
‡ Argonne National Laboratory.

High Pressure Pyrolysis of Toluene

J. Phys. Chem. A, Vol. 110, No. 30, 2006 **9389**

Recent experimental and modeling studies[17,18] in this laboratory at high pressures and high temperatures on the oxidation of toluene have highlighted the dominant role of these primary dissociation rates at high temperatures (>1200 K). To better isolate the contributions of these primary pyrolytic channels we have initiated the current study of toluene pyrolysis. The current paper forms part 1 of a two-part series on toluene pyrolysis that discusses the experimental measurements as well as the modeling of toluene, benzene, and methane profiles from the HPST in combination with temporal H atom ARAS profiles from prior shock tube experiments to extract high-pressure limit dissociation rate constants for the two primary channels. Part 2 in this series[19] discusses the modeling of benzyl decomposition as well as the growth of key soot precursors such as C_2H_2, C_4H_2, C_8H_6, and indene.

Experimental and Analytical

The UIC high-pressure shock tube (HPST) is operated as a single pulse shock tube with experiments performed behind reflected shock waves. The design and operation of the shock tube have been described in detail in earlier publications,[20-22] and the present toluene pyrolysis experiments were performed with only minor changes to the setup that involve the use of heated sample vessels, mixture rig, and analytical rig.

The present sets of experiments were performed with a 101 in. long driven section with the diaphragm section separating it from a 60 in. long driver section. The driver section length is made variable by the insertion of brass plugs in order to obtain best possible cooling rates (7×10^4 to 1.5×10^5 K/s). A dump tank placed just ahead of the diaphragm section on the driven side rapidly quenches the reflected shock wave, thereby permitting the shock tube to be operated in single pulse fashion. Incident shock velocities were calculated from the response of pressure transducers (PCB model Nos. 113A23 [0−10000 psi] and 113A21 [0−200 psi]) located in the side wall of the shock tube perpendicular to the incident shock wave and these velocities have been correlated with the temperature in the reaction zone using the chemical thermometer technique.[21,22] Uncertainty in the measured shock velocities is ≤1%. These shock velocities have been calibrated to the reaction temperature by measuring the extent of decomposition of a chemical calibrant (1,1,1-trifluoroethane) which has a well-established k_∞.[21] Effects due to pressure rise/drop and quench time have been analyzed and found to be insignificant.[21] Consequently the uncertainty in temperature is estimated to be no more than 1% over the temperature range of the present experiments. Reaction pressures and reaction times[20-22] are obtained from a pressure trace recorded from a pressure transducer mounted in the end wall of the driven section parallel to the long axis of the shock tube. The present set up gave reaction times in the range 1.2−1.5 ms with exact reaction times measured for each experiment. Uncertainty in the time measurement is no more than 10%. Prior to each experiment, the driven and the sampling sections of the shock tube were evacuated to 1×10^{-5} Torr by means of two sets of rotary-pump (Edwards E2M-1.5)/turbo-pump (Edwards EXT-250HI) combinations, and a separate rotary pump (Edwards RV-8) was used to evacuate the driver section.

Reagent mixtures consisting of toluene, 104 ppm (99.8%+, Aldrich Chemical Co.) and neon, 2400 ppm (Grade 5.0, 99.999%, BOC Gases) diluted in the bath gas, argon (Grade 5.0, 99.999%, BOC Gases) were prepared manometrically in 50 L vessels and allowed to stand overnight before use. A freeze−thaw procedure was used before admitting toluene into the mixture vessel to minimize air content whereas the permanent gases were used as obtained. Neon was added as an internal standard[21] in the experiments to account for any dilution of post-shock gases by the driver gas (helium, Grade 4.8, 99.99%, BOC Gases).

Pre- and postshock samples were withdrawn into electropolished stainless steel vessels via a port located in the endwall of the shock tube and analyzed offline using standard gas chromatographic (GC) and mass spectrometric (MS) techniques. The analyses were performed by simultaneously injecting the gas samples via gas sampling valves onto three columns. Two PLOT-Q columns on two GC's (HP-6890) with one column eluting into a FID and the other into a MS (HP-5973) were used to analyze the hydrocarbons. A MOLSIEVE 5A column eluting into a TCD was used for analyzing neon. Excellent baseline separation was achieved for all the observed intermediates. Multiple analysis runs were performed for a few experiments (typically one to two experiments every day) to ensure that the data was consistent and reproducible (typically within ±5%), in line with prior work from this laboratory.[17,22] Identification of reaction products was achieved by retention time matching as well as with the aid of the MS. The detectors were calibrated using calibration standards and makeup mixtures (that span the low mole fraction regime 1−100 ppm, as in the current experiments) and the calibrations were checked periodically for consistency. Uncertainties in species mole fractions are estimated to be no more than 5%, typical error bars for GC, GC-MS measurements.

Experimental Results

Toluene pyrolysis experiments were performed over a wide temperature range from 1200 to 1900 K. A total of 72 experiments were performed at two nominal pressures of 27 (37 experiments) and 45 bar (35 experiments). The diaphragm opening process causes minor variations (±10% from nominal pressures) in the final pressures attained, and consequently, we refer to the experiments being performed at the nominal pressures quoted above. However the exact reaction pressures for each experiment are shown in the Supporting Information, Table ST1, and these have been used for all the simulations that have been performed in this work. The reaction times for these experiments were in the range 1.5 ± 0.2 ms (again due to the shock conditions and the nature of the shock quenching process). Experiments were performed using dilute toluene mixtures with mole fractions of 104 ppm that translate to initial concentrations that range from 1.8×10^{-8} to 4.9×10^{-8} mol/cm^3. The low mole fractions minimize temperature drop due to endothermicity, less than 5 K, thereby maintaining essentially isothermal conditions over the time range (1.3−1.7 ms) of the current experiments. A number of intermediates were observed in these experiments principal among these being the smaller hydrocarbons C_6H_6 (benzene), C_2H_2, CH_4, C_4H_2 (diacetylene), C_4H_4 (vinylacetylene) 1,3-C_4H_6 (1, 3-butadiene), C_2H_6, allene, propyne, and the small aromatics phenylacetylene, styrene, *p*-xylene, ethylbenzene, and indene. The carbon totals in these experiments were poor at the higher temperatures beyond 1600 K with carbon recoveries being close to 50% (See Supporting Information, Table ST1, for carbon recoveries for each experiment). Formation of small amounts of single ring aromatics and the smallest five and six member ring PAH, indene, in the present experiments offer ample evidence of the presence of heavier aromatics and polycyclics in small amounts that could be condensed on the walls of the shock tube. Furthermore, it is well-known that acetylene and diacetylene formation lead to subsequent larger polyacetylenes (C_6H_2, C_8H_2) which might

explain the poor carbon balance. The species profiles for the two sets of experiments at 27 and 45 bar are shown in Figures 1 and 2.
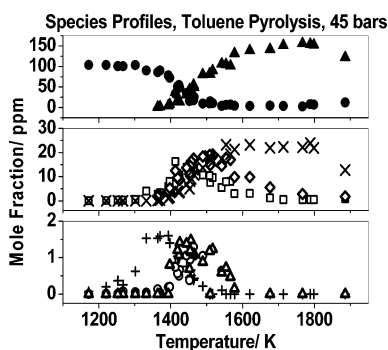
Figure 1. 45 bar species profiles. [●] − $C_6H_5CH_3$, [□] − C_6H_6, [▲] − C_2H_2, [◊] − CH_4, [X] − C_4H_2, [+] − C_8H_{10}, [○] − C_8H_6, [△] − C_9H_8.
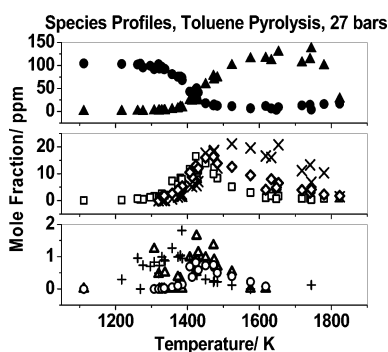
Figure 2. 27 bar species profiles. [●] − $C_6H_5CH_3$, [□] − C_6H_6, [▲] − C_2H_2, [◊] − CH_4, [X] − C_4H_2, [+] − C_8H_{10}, [○] − C_8H_6, [△] − C_9H_8.

Both sets of experiments exhibit very similar profiles. Toluene starts to decay at temperatures above 1300 K. Correspondingly, benzene and CH_4 start to build up and attain their maxima at temperatures close to 1460 and 1520 K respectively. C_2H_2 and C_4H_2 build up to significant amounts and only at temperatures beyond 1700 K start to get consumed. 90% of the toluene is consumed at temperatures close to 1500 K. C_2H_2 is the most dominant intermediate with as much as 150 ppm being formed in these experiments. The single ring aromatics, phenylacetylene, styrene, ethylbenzene, and *p*-xylene, as well as the largest aromatic species sampled in the current study, indene (C_9H_8), were formed in significantly smaller quantities with mole fractions being no more than 2 ppm. The raw experimental data sheets with mole fractions for all the intermediates that were detected in quantifiable amounts along with the experimental parameters (P_5, T_5, and t) are included in the Supporting Information, Table ST1.

The experimental data was used to obtain overall rate constants for the decay of toluene using first-order kinetics (eq 1). Figure 3 shows the overall decay rate coefficients obtained for the 27 and 45 bar experiments.

$$k_{Total} = \frac{\ln(1-x)}{t} = A \exp\left(\frac{-E_a}{RT}\right) \quad (1)$$

$$\text{where } x = \frac{[C_6H_5CH_3]_i - [C_6H_5CH_3]_f}{[C_6H_5CH_3]_i}$$

The species profiles (Figures 1 and 2) indicate clearly that the majority of the reactant (>95%) is consumed at temperatures close to 1500 K and correspondingly the rate coefficients would

show significant curvature and flattens out at higher temperatures as can be seen in Figure 3a. The decay rate coefficients shown in Figure 3b are consequently plotted only for experiments in the temperature range 1171−1509 K and this corresponds to 47 out of the total of 72 experiments being used to obtain the total toluene decay rate parameters. Figure 3b indicates that there is no significant pressure dependence over the temperature range. A linear least-squares fit to the data was obtained with a good correlation coefficient ($R^2 = 0.97$). The extracted Arrhenius parameters, the preexponential A factor (8.67×10^{14}/s) and the activation energy E_a (79550 cal/mol) are also shown in the figure. A variability in reaction time by 10% as well as species mole fraction by 5% has a minimal effect on the estimated total decay rate constants. On the other hand a 1% variation in reaction temperature leads to a 50% change in the determined rate constants. This translates to uncertainties of ±1 kcal/mol and ±10% for the derived overall E_a and A factors, respectively.
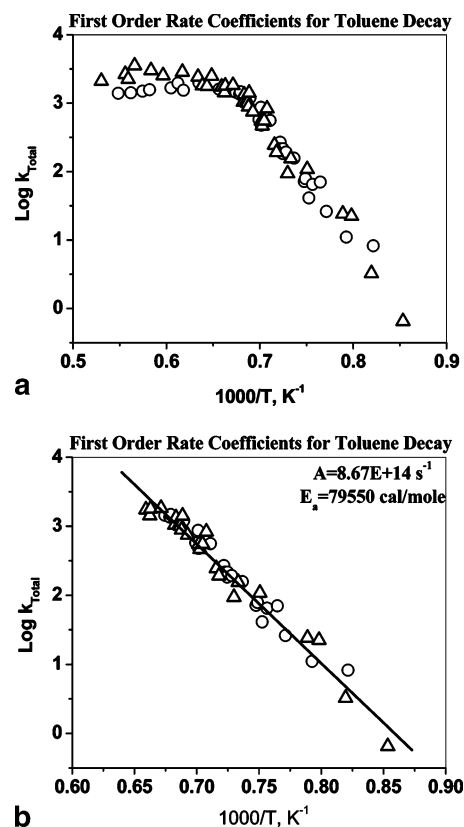
Figure 3. First-order total decay rate coefficients. [○] − 27 bar decay rate coefficients, [△] − 45 bar decay rate coefficients, [—] − 27 and 45 bar combined linear fit.

Figure 4 shows the comparison of reported literature rate coefficients to the current extracted rate constant from the HPST (circles denote the extracted rate constants that have been obtained from the Arrhenius parameters in Figure 3). The NIST chemical kinetics database[23] mentions five prior measurements[7,13,24−26] of rate constants derived for $C_6H_5CH_3 \rightarrow$ products. Among these five studies, the mass spectrometric study by Smith[7] does not report any rate constants. Astholz and Troe[24] studied the decomposition of benzyl radicals using toluene as a source for benzyl radicals and reported rate constants for benzyl decay to form products ($C_6H_5CH_2 \rightarrow$ products). These rate constants/rate parameters have been erroneously ascribed to the $C_6H_5CH_3 \rightarrow$ products reaction in the NIST database. The study by Hippler et al.[13] on toluene and benzyl pyrolysis was used to estimate k_∞ for $C_6H_5CH_3 \rightarrow C_6H_5CH_2 + H$ (−1b) over the
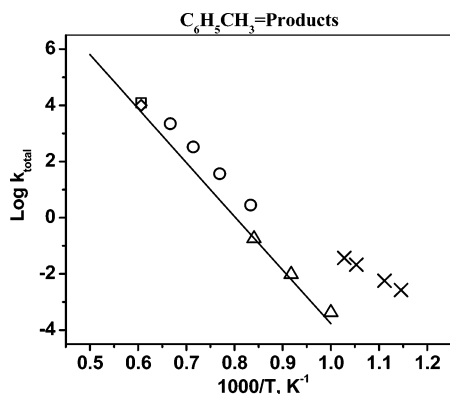
High Pressure Pyrolysis of Toluene

J. Phys. Chem. A, Vol. 110, No. 30, 2006 **9391**

Figure 4. Comparison of total toluene decay rate coefficients. [O] − HPST (1200−1500 K), [□] − Kern et al.[15] (1650 K), [△] − Bruinsma et al.[26] (1090−1190 K), [◇] − Eng et al.[27] (1650 K), [X] − Banerjee et al.[25] (875−975 K) [—] − Baulch et al.[29] (1000−2000 K).

temperature range 1200−1500 K. The NIST database has again erroneously ascribed the rate constants for this reaction to be the same as that for $C_6H_5CH_3 \rightarrow$ products. Hippler et al. [13] in their study have assumed that over their temperature range there is no contribution from the other toluene dissociation channel via $C_6H_5CH_3 \rightarrow C_6H_5 + CH_3$ (−1a). The other two studies by Bruinsma et al.[25] and Banerjee et al.[26] using flow reactors have reported first-order rate constants for $C_6H_5CH_3 \rightarrow$ products at temperatures < 1200 K. The present study appears to be the only high-temperature measurements for $C_6H_5CH_3 \rightarrow$ products. Considering that very dilute mixtures were used in our study and the temperature range over which the rate coefficient for toluene decomposition was obtained in the present work, 1200 to 1500 K and pressures > 20 atm (total Ar densities 10^{-4} mol/cm³) the total rate reported here is a true first-order high-pressure

limiting decay rate, k_∞, and there appears to be no indication of falloff in the current experiments in line with calculations reported in a number of earlier studies.[13,27,28]

The rate constants derived from the present work appear to be larger than a factor of 2 than those reported in the recent work by Eng et al.[27] Eng et al.[27] have reported fall off curves (Figure 6 in their paper) and branching ratios (Figure 7 in their paper) for toluene decomposition at temperatures of 1650, 1850, and 2000 K. Here the sum of the rate constants for reactions −1a and −1b from Eng et al.[27] were taken to represent total toluene decomposition. For example at 1650 K and total shock densities of 3.7×10^{-4} mol/cm³ ($P = 50$ atm), $k_{uni} = k_{-1a} + k_{-1b}$ appears to be at the high-pressure limit with a magnitude just larger than 9.9×10^3/s. If one were to use our total first-order decay rate parameters (Figure 3b) $k_{uni,\infty}$ is calculated to be 2.5×10^4/s, a factor of 2.5 larger. However one should note that our rate constants are representative of total decay rate constants for $C_6H_5CH_3 \rightarrow$ Products and on the other hand the Eng et al.[27] rate constant refers to the sum of rate constants for reactions −1a and −1b. Despite this one could argue that the match between the Eng et al.[27] predictions and our experimental rate constants is good.

One other point to note is that branching ratios derived from the Eng et al.[27] work appear to support the dominance of reaction −1b with reaction −1a appearing to be equally dominant only at 2000 K at total Ar densities > 10^{-4} mol/cm³. This is in marked contrast to the detailed experimental and modeling studies by Pamidimukkala et al.[9] and Kern et al.[15] Kern et al.[15] have concluded that the magnitude of the rate constants for both the initiation reactions (−1a and −1b) in toluene are comparable in the temperature range 1400−1600 K with the phenyl channel (−1a) dominating at higher temperatures on the basis of detailed modeling of the available experiments. Kern et al.[15] have derived
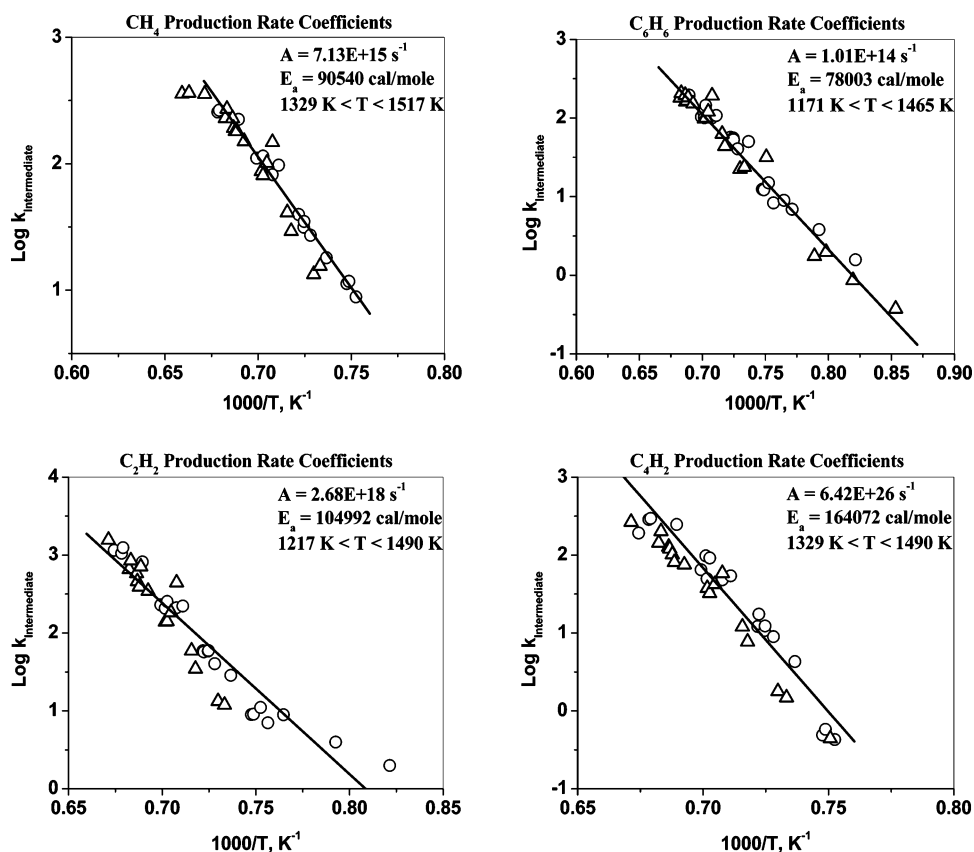

Figure 5. Production rate coefficients. [O] − 27 bar decay rate coefficients, [△] − 45 bar decay rate coefficients, [—] − 27 and 45 bar combined linear fit.

TABLE 1: First Order Decomposition and Production Rate Parameters

species	log (A, s^{-1})	E_a (kcal/mole)	temp range (K)
toluene	14.94 ± 0.05	79.6 ± 1	1171−1509
methane	15.85 ± 0.05	90.5 ± 1	1329−1517
benzene	14.00 ± 0.05	78.0 ± 1	1171−1465
acetylene	18.43 ± 0.05	105.0 ± 1	1217−1490
diacetylene	26.81 ± 0.05	164.1 ± 1	1329−1490

pressure dependent rate constants for both the reactions. If one were to use the Eng et al.[27] approach in summing up the rate constants for the two reactions −1a and −1b from the pressure dependent rate parameters from Kern et al.[15] and reporting that as the total rate constant for toluene decay one would obtain again at 1650 K $k_{uni} = k_{-1a,\infty} + k_{-1b,\infty} = 1.23 \times 10^4$/s (a factor of 2 less than the current HPST rate constant at 1650 K) at total shock densities of 3.7×10^{-4} mol/cm^3 ($P = 50$ atm). This is in good agreement with the HPST measurements. Again one should reassert that, among the studies considered here, the derived rate constants from the HPST study represent true k_∞ considering the experimental conditions of the present work, on the other hand the Eng et al.[27] and the Kern et al.[15] experiments are in the falloff regime with k_∞ derived from extrapolations to their data. The present rate coefficients also compare favorably (being less than a factor of 2) against those from the extrapolated lower temperature flow tube measurements of Banerjee et al.[25] in the 1200−1250 K temperature range but the deviations increase at higher temperatures being as much as an order of magnitude at 1500 K. On the other hand the measurements for total decay rate coefficients by Bruinsma et al.[26] are an order of magnitude or more smaller than the current measurements over the temperature range 1200−1500 K. The recent recommendations by Baulch et al.[29] for $k_{-1a,\infty} + k_{-1b,\infty}$ appear to be lower by a factor of 2 (at 1650 K) than the current measurements as well as the Eng et al.[27] and Kern et al.[15] recommendations with increasing deviations at lower temperatures (being as high as an order of magnitude at 1200 K).

The total decay rate coefficients for the decomposition of toluene have also been used to extract production rate coefficients (using eq 2, see for example ref 30) for the formation

$$k_{Intermediate} = \frac{[Intermediate]_i}{[C_6H_5CH_3]_i - [C_6H_5CH_3]_f} \times k_{Total} \quad (2)$$

of the dominant species in the current experiments viz. C_6H_6, CH_4, C_2H_2, and C_4H_2. Figure 5 depicts the total production rate coefficients for the formation of the major intermediates from the current experiments. No significant pressure dependency is observed as can be seen in Figure 5. The total production rate coefficients for both high-pressure data sets have been fit to the Arrhenius expression with a good correlation coefficient (∼0.95) to extract the preexponential factor (A) and the activation energy (E_a). Production rate coefficients have been extracted over the lower temperature range of the experiments before subsequent decay of the intermediates occur. Table 1 summarizes the extracted Arrhenius parameters for the decomposition rate of the reactant, toluene, as well as production rates for the various intermediates. The extracted Arrhenius parameters are not representative of true first-order kinetics. However they represent a useful measure to summarize global formation rates.[30]

Modeling

Despite a number of experimental and modeling studies on toluene dissociation at high temperatures there still exist discrepancies in several key features pertaining to its mechanism. A majority of the earlier higher temperature toluene dissociation studies[10,11] assumed the dominance of the benzyl channel (1B) at temperatures as high as 1800 K and the rate coefficients for the primary reactions (−1a and −1b) were extracted in these experiments by means of modeling absorption profiles of toluene, benzyl, and benzyl fragments as well as H atom profiles. However experimental and subsequent detailed modeling studies by Pamidimukkala et al.[9] and Kern et al.[15] have concluded that reaction −1a dominates at temperatures as low as 1400 K. They derived their conclusions by modeling shock tube laser−schlieren (LS) profiles to obtain precise initial rate coefficients that equate to total rate coefficients for reactions −1a and −1b. Additionally shock tube time-of-flight (TOF) methane profiles were used to derive branching ratios for the two channels. Kern et al.[15] were also able to model H atom profiles measured by Braun-Unkhoff et al.[10] fairly accurately with the extracted high-temperature rate coefficients.

Conversely, recent studies on the decomposition of toluene[27] behind shock waves using atomic resonance absorption spectroscopy (ARAS) to detect H atoms in combination with subsequent master equation simulations support earlier conclusions[10,11] that temperatures > 2000 K are required at the high-pressure limit in order for −1a to be equally dominant to −1b. The rate constants for channel −1b are fairly accurately known on the basis of lower temperature measurements < 1150 K[31] where only the benzyl channel predominates. On the other hand, isolation of the phenyl channel is extremely difficult at high temperatures and consequently one is forced to resort to modeling of CH_4 profiles to indirectly extract rate coefficients for the phenyl channel (−1a). To unambiguously extract rate coefficients for −1a theory appears to be the only recourse.

In recent work, Harding and Klippenstein[32a,b] have directly implemented multireference wave function based methods (MRCI/CASPT2) within variable reaction coordinate transition state theory (VRC-TST) for the key association reactions (1a, 1b) to yield a pressure dependent

$$CH_3 + C_6H_5 \rightarrow C_6H_5CH_3 \quad (1a)$$

$$H + C_6H_5CH_2 \rightarrow C_6H_5CH_3 \quad (1b)$$

analysis of the primary rate coefficients in toluene decomposition over a wide range of temperatures (100−2658 K). The current experiments have been performed at high pressures and consequently we have utilized only the high-pressure limiting rate coefficients from the Klippenstein et al.[32a,b] calculations for our kinetic analysis. Apart from these steps (−1a and −1b represent the primary dissociation steps for toluene) the chemical kinetic model that has been assembled to describe toluene pyrolysis includes key steps that describe abstraction reactions with H and CH_3, benzyl decomposition reactions, a benzene decomposition submechanism, reactions that describe the formation and consumption of smaller hydrocarbons that range from methane to cyclopentadiene and reactions that describe the formation of key single ring aromatic soot precursors such as phenylacetylene and indene. The assembled model incorporates 87 species and 262 reactions. Large parts of the model that involve the formation and consumption of smaller hydrocarbons (C_1−C_5) are based on the Princeton toluene model.[33,34] The model however does not incorporate reactions for the formation and consumption of single ring aromatics, and consequently in this work, we have included 81 reactions that describe their formation discussed in great detail in part 2 of this series.[19] Apart from these additions, several changes have been made to key steps

High Pressure Pyrolysis of Toluene

J. Phys. Chem. A, Vol. 110, No. 30, 2006 **9393**

TABLE 2

reaction	A	n	E_a	
$CH_3 + C_6H_5 \rightarrow C_6H_5CH_3$	4.601×10^{14}	-0.33756	0	(fit to HK rate 1027 K < T < 1897 K)
reverse	9.130×10^{27}	-3.330	107 992	(thermochemistry from ref 36)
$H + C_6H_5CH_2 \rightarrow C_6H_5CH_3$	5.384×10^{13}	0.113 05	0	(fit to HK rate 1027 K < T < 1897 K)
reverse	3.346×10^{15}	0.17	91 409	(thermochemistry from ref 35)

in toluene decomposition (incorporating updated Baulch et al.[29] recommendations) that are outlined in more detail later in this article.

Primary Reactions

The two primary decomposition channels in toluene, reactions $-1a$ and $-1b$, represent the most dominant and sensitive channels that not only govern the rate of decomposition of toluene but also significantly affect the formation of subsequent key intermediates. Harding and Klippenstein [HK, ref 32] have obtained high-pressure limiting association rate coefficients, k_{1a} and k_{1b}, from their master equation calculations over a wide temperature range that spans $100-2658$ K of which the range $1027-1897$ K is relevant to the current work. Consequently, we have chosen to fit k_{1a} and k_{1b} over the temperature range $1027-1897$ K by a modified Arrhenius expression to take into account the moderate temperature dependence that is exhibited for the two barrierless reactions. k_{-1a} and k_{-1b} are obtained over the same temperature range from these association rate coefficients via the equilibrium constants using the most recent thermochemical information for the benzyl radical[35] and the phenyl radical[36] for which the heat of formation is based on the recommendation by Davico et al.[37] These two radicals have the largest uncertainties in their heats of formation, ΔH_f^0, among the species in reactions 1a and 1b (the heats of formation for these two radicals have a significant effect on the equilibrium constant and consequently the reverse rate coefficients for 1a and 1b). The reverse rate constants were calculated from the forward rate constants and the thermochemical parameters[35,36] using CHEMREV.[38] The forward and reverse rate parameters for the two channels are shown in Table 2 (units in cal, mole, s). Using these rate parameters the branching ratios for the two channels vary from 0.04 at 1200 K to 0.10 at 1800 K. Here the branching ratios are defined as $(k_{-1a,\infty})/(k_{-1a,\infty} + k_{-1b,\infty})$.

A cause for concern with regard to the thermochemistry for large radicals such as the benzyl and phenyl radicals is the large number of low frequency vibrational modes that contribute significantly to the thermochemical functions (H, C_p, S) when extrapolated to temperatures >1000 K. In the case of the benzyl radical we have used the IUPAC recommendation[35] in which vibrational frequencies from DFT calculations at scaled B3LYP/6-31G(d) level of theory and the CH_2 torsional mode (485 cm^{-1}) treated as a hindered rotor with a torsional barrier height of 46.4 kJ/mol have been used to obtain the thermochemical functions, over a wide temperature range from 50 to 6000 K. Additionally we have performed higher level DFT calculations (B3LYP/6-311++G(d,p) level of theory) and compared the thermochemical parameters obtained from these vibrational frequencies with those from the IUPAC data sets for the benzyl radical. Over the temperature range of interest, $1000-2000$ K, the differences are no more than a 0.5 cal/(mol K) difference in C_P and S and no more than 0.5 kcal/mol difference in $H(T) - H(0)$, which translates to a less than 10% deviation when calculating reverse rate coefficients. Consequently, to estimate the thermochemical properties in the remainder of the article, we have used the vibrational frequencies reported in the IUPAC compilation. Additionally the effect of replacing the restricted rotor model in benzyl with the simpler rigid rotor harmonic

oscillator (RRHO) model has been examined and again the effect is minor for this species and the RRHO model has been used throughout. In the case of the other key radical, the phenyl, there are no internal rotors and very few low-frequency vibrations (with the lowest vibrational frequency ~ 400 cm^{-1}) and consequently the all frequencies RRHO formalism is adequate for extrapolating the thermochemical functions.

The calculated primary forward and reverse rate parameters and thermochemistry were inserted into the detailed model of toluene pyrolysis and used in a multistep modeling approach to fit H atom ARAS profiles measured by Braun-Unkhoff et al.[10] and Eng et al.[27] as well as key intermediate species profiles (CH_4 and C_6H_6) from the current high-pressure single pulse shock tube experiments (attached as Supporting Information in Table ST1). The simulations were performed using the SENKIN program within the CHEMKIN[39] suite. Figure 6 represents the comparison of model simulations and experimental H atom profiles. Short time scales ($<200-300$ μs) represent the most important regime in these ARAS experiments when there are minimal contributions due to secondary chemistry, and fairly unambiguous rate coefficients for primary reactions can be extracted (as long as dilute mole fractions of the fuel are utilized).

In general, good agreement can be obtained between the experimental H atom profiles and the model simulations in the short time scale regime (<300 μs) where the contributions are primarily due to only the two primary channels 1A and 1B with no significant effects of secondary chemistry. A more stringent test for the model incorporating the calculated association and dissociation rate coefficients, specifically for channel 1A, lies in their predictive capability for methane and benzene profiles. In the present high-pressure single pulse shock tube experiments, we have measured detailed profiles that depict CH_4 and C_6H_6 formation and decay over the temperature range $1100-1900$ K (see Figures 2 and 3 above). Figure 7 depicts the predictions made by the detailed model (Table ST2) with the same primary rate coefficients as for the H atom simulations shown in Figure 6. The model appears to match the toluene decay profiles only moderately well and the peak methane mole fraction as well as the profile over the entire temperature range of the experiments is under predicted by a factor of 2 or larger. A similar trend is observed for the benzene profiles for which the model predictions are shifted from the data over the entire temperature range. Sensitivity analyses (see Figure 8) performed for the three species clearly highlight the importance of the primary rate coefficients as well as H and CH_3 concentrations using the detailed model for a representative shock at 1500 K and 45 bars. Specifically for CH_4 concentrations the primary channel 1A, as well as reactions between H atoms and toluene depict the maximum sensitivity. The rate coefficients for the two major channels for the reaction between H and $C_6H_5CH_3$ forming $C_6H_5CH_2 + H_2$ and $C_6H_6 + CH_3$ have been set to the Baulch et al.[29] and Robaugh and Tsang[40] recommendations, respectively. The rate coefficient for H abstraction from toluene forming the *p*-methylphenyl was taken from Kiefer and Kern[9,15] and is probably an upper limit since they have lumped the three methylphenyls (ortho, meta, and para) as a single species in their model. The only other sensitive reaction, apart from eq
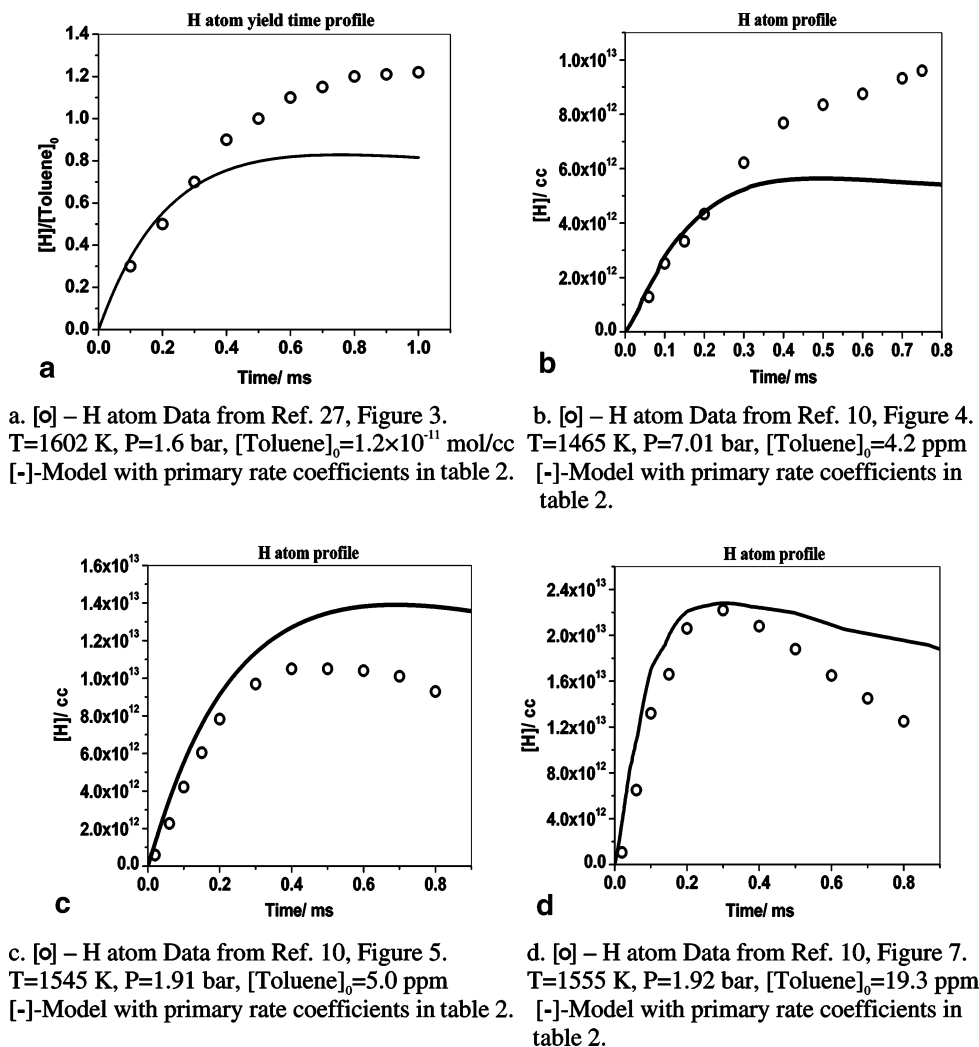
a. [o] – H atom Data from Ref. 27, Figure 3.
T=1602 K, P=1.6 bar, [Toluene]$_0$=1.2×10^{-11} mol/cc
[-]-Model with primary rate coefficients in table 2.

b. [o] – H atom Data from Ref. 10, Figure 4.
T=1465 K, P=7.01 bar, [Toluene]$_0$=4.2 ppm
[-]-Model with primary rate coefficients in
table 2.

c. [o] – H atom Data from Ref. 10, Figure 5.
T=1545 K, P=1.91 bar, [Toluene]$_0$=5.0 ppm
[-]-Model with primary rate coefficients in table 2.

d. [o] – H atom Data from Ref. 10, Figure 7.
T=1555 K, P=1.92 bar, [Toluene]$_0$=19.3 ppm
[-]-Model with primary rate coefficients in
table 2.

Figure 6. H atom profiles from shock tube−ARAS experiments.
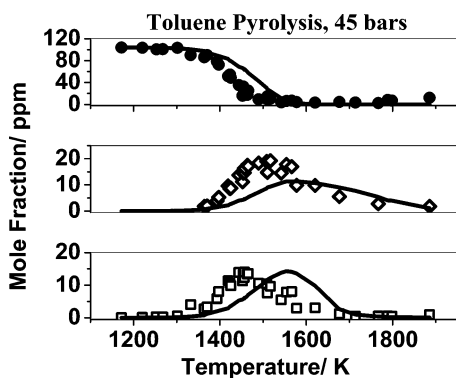
Figure 7. HPST profiles. [●] − $C_6H_5CH_3$, [□] − C_6H_6, [◇] − CH_4, [—] − detailed model.

−1a, (among the 262 reactions in the detailed model) is the reaction, $C_6H_5CH_3$ + CH_3 → $C_6H_5CH_2$ + CH_4 (reaction 174 in the Supporting Information, Table ST2)

There is an order of magnitude scatter in the intermediate temperature regime spanning 600−1000 K in the reported literature rate coefficients for reaction 174. There are no higher temperature measurements and one might expect significant non-Arrhenius dependence for the rate of this reaction at the temperature range of interest in this study ∼1200−1600 K. The estimate made by Kern et al.[15] for the rate coefficient of this reaction at high temperatures is higher by a factor of 2−3 (over the temperature range 1200−1600 K) than the highest literature

rate coefficients measured by Price and Trotman-Dickenson.[41] Another point to be noted is that the literature rate coefficients for reaction 174 were measured 15−50 years ago relative to other reference reactions such as CH_3 + CH_3 = C_2H_6 and C_2H_4 + CH_3 = C_2H_3 + CH_4, making it a complex task to evaluate these measurements.

We have estimated high-temperature rate constants for reaction 174 on the basis of the recent Baulch et al.[29] recommendations for the rate coefficients for $C_6H_5CH_3$ + H = $C_6H_5CH_2$ + H_2, C_2H_6 + H = C_2H_5 + H_2 and C_2H_6 + CH_3 = C_2H_5 + CH_4 which have reported uncertainties of no more than a factor of 2 at high temperatures (1500 K). Over the temperature range 1000−1800 K, the rate constants for C_2H_6 + CH_3 = C_2H_5 + CH_4 vary by a factor of 0.01−0.23 relative to the rate constants for C_2H_6 + H = C_2H_5 + H_2. We have applied the same factors to the literature rate coefficients for $C_6H_5CH_3$ + H = $C_6H_5CH_2$ + H_2 to estimate the rate constants for C_6H_5-CH_3 + CH_3 = $C_6H_5CH_2$ + CH_4 over the temperature range 1000−1800 K. The estimated rate constants over this temperature range were then fit to a non-Arrhenius expression and these (see Table ST2 attached as part of the Supporting Information for detailed model) are 4.5−6.5 times higher than the rate constants used by Kern et al.[15] in the temperature regime 1200−1600 K. This estimated value is probably an upper limit and with these rate constants in the assembled model the CH_4 profiles remain under predicted as can be seen in Figure 7. The CH_3/CH_4 and C_6H_6 profiles are insensitive to the small molecule
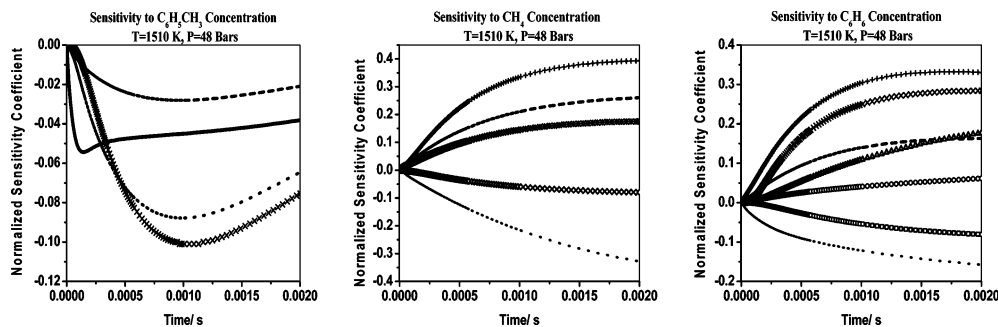
High Pressure Pyrolysis of Toluene

J. Phys. Chem. A, Vol. 110, No. 30, 2006 **9395**

Figure 8. Sensitivity analyses. [—] − H + $C_6H_5CH_2$=$C_6H_5CH_3$, [---] − CH_3 + C_6H_5=$C_6H_5CH_3$, [···] − $C_6H_5CH_3$ + H=$C_6H_5CH_2$ + H_2, [+] − $C_6H_5CH_3$ + H=C_6H_6 + CH_3, [*] − $C_6H_5CH_3$ + CH_3=$C_6H_5CH_2$ + CH_4, [×] − $C_6H_5CH_2$=C_5H_5 + C_2H_2, [△] − C_3H_3 + C_3H_3=C_6H_6, [○] − C_6H_6=C_6H_5 + H, [□] − C_6H_6 + H=C_6H_5 + H_2, [◇] − $C_6H_5CH_3$ + H=p-$C_6H_4CH_3$ + H_2.

TABLE 3

reaction	A	n	E_a
$CH_3 + C_6H_5 \rightarrow$ $C_6H_5CH_3$	4.601×10^{14}	-0.33756	0 (fit to HK rate 1027 K $< T < 1897$ K)
reverse	4.620×10^{25}	-2.530	104483 ($\Delta H_f^0{}_{298K}$ C_6H_5 = 78.6 kcal/mol)

chemistry (C_1−C_3). The only C_3 reaction to which the benzene profiles show any significant sensitivity is as expected, the propargyl recombination reaction. Given the sensitivity of this reaction, the rate coefficient in the model is based on recent measurements (see Table ST2). The model also includes updated thermochemistry for the important CH_3 radical from the IUPAC tables published recently.[35] Consequently the only channel of consideration for the CH_4 profiles appears to be the primary channel 1A (association reaction 1a and the corresponding reverse dissociation reaction −1a).

The heat of formation for the phenyl radical plays a dominant role in determining the equilibrium constant for channel 1A and since this channel has the most effect on the simulation of the methane profiles, the heat of formation of phenyl was examined further. Davico et al.[37] have recommended the value for ΔH_f^0-(300 K) for the phenyl radical to be 81.2 ± 0.6 kcal/mol and this is the value that has been used to extract the rate coefficient for reaction −1a in the model. However there is significant uncertainty in the reported heats of formation for the phenyl radical with recent studies that recommend values between 78 and 80 kcal/mol.[42] These numbers are more in line with the recommendation of McMillen and Golden[43] (in comparison to the higher value reported by Davico et al.[37]) who have used a third-law analysis to derive the ΔH_f^0(298K) for C_6H_5 to be 78.6 $\pm$ 2 kcal/mol. On the basis of these recommendations[42,43] we have used the lower value (78.6 kcal/mol) for the ΔH_f^0(298K) of C_6H_5 to back out the reverse rate coefficients for channel 1a (again with the forward association rate coefficients of HK over the temperature range 1027−1897 K). This value is also within the error bars quoted by Kiefer et al.[44] who have derived ΔH_f^0-(298K) for C_6H_5 to be 80 ± 2 kcal/mol from their laser schlieren benzene pyrolysis experiments. The derived reverse rate coefficients (rate parameters shown below) are 6.5−5.5 times higher than the rate coefficients derived using the higher heat of formation for the phenyl radical. This represents a significant change and we have used these (Table 3, units in cal, mole, s) forward and reverse rate coefficients in the model with no other change made to any of the other rate coefficients or thermochemical parameters. Figure 9 shows the predictive capability of the model for the single pulse shock tube species profiles with the updated thermochemistry for the phenyl radical. There is a much improved fit for the methane and benzene profiles, specifically at temperatures <1550 K where the fit is excellent at which point more than 95% of the toluene has decomposed.
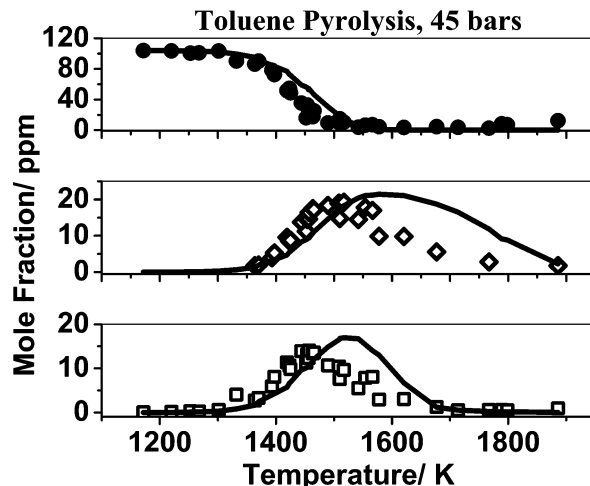

Figure 9. HPST profiles: (●), $C_6H_5CH_3$; (□) C_6H_6; (◇) CH_4; (-) detailed model.

The same model with the modified phenyl heat of formation ($\Delta H_f^0{}_{298K} = 78.6$ kcal/mol) was used to predict the ARAS H atom profiles for the experiments depicted in Figure 6a−d. Parts a−d in Figure 10 show the predictions made by the model to the H atom temporal profiles.

The predictive capability of the model for H atoms has significantly worsened with the updated heat of formation for the phenyl radical used to obtain Figure 9. Here the phenyl channel plays a more dominant role with branching ratios varying from 0.22 at 1200 K to 0.37 at 1800 K. However we have already shown that this change in the heat of formation for phenyl is essential in order to simulate our single pulse shock tube profiles. Sensitivity analysis performed for the H atom concentrations shown in Figure 11, parts a and b, for the experiments in Figure 10, parts a and c, reveal that the only channels that exhibit significant sensitivity at short times (<200 μs) are the two primary channels. The rate coefficient/equilibrium for channel 1A cannot be changed without affecting the excellent fits to the single pulse shock tube methane and benzene profiles.

As with reaction 1a, reaction 1b is also a radical−radical addition reaction, and consequently, the thermochemistry for the species in this reaction needs to be well validated in order to obtain precise equilibrium constants for channel 1B. With the thermochemical parameters for $C_6H_5CH_3$ and H being well established, $C_6H_5CH_2$ appears to be the species with the largest uncertainty. The recent IUPAC recommendation[35] for the benzyl radical is based on a detailed review of existing data. However the review does not incorporate the detailed toluene and benzyl dissociation studies of Braun-Unkhoff et al.[10,28] Braun-Unkhoff et al.[10] have studied H atom formation from toluene dissociation
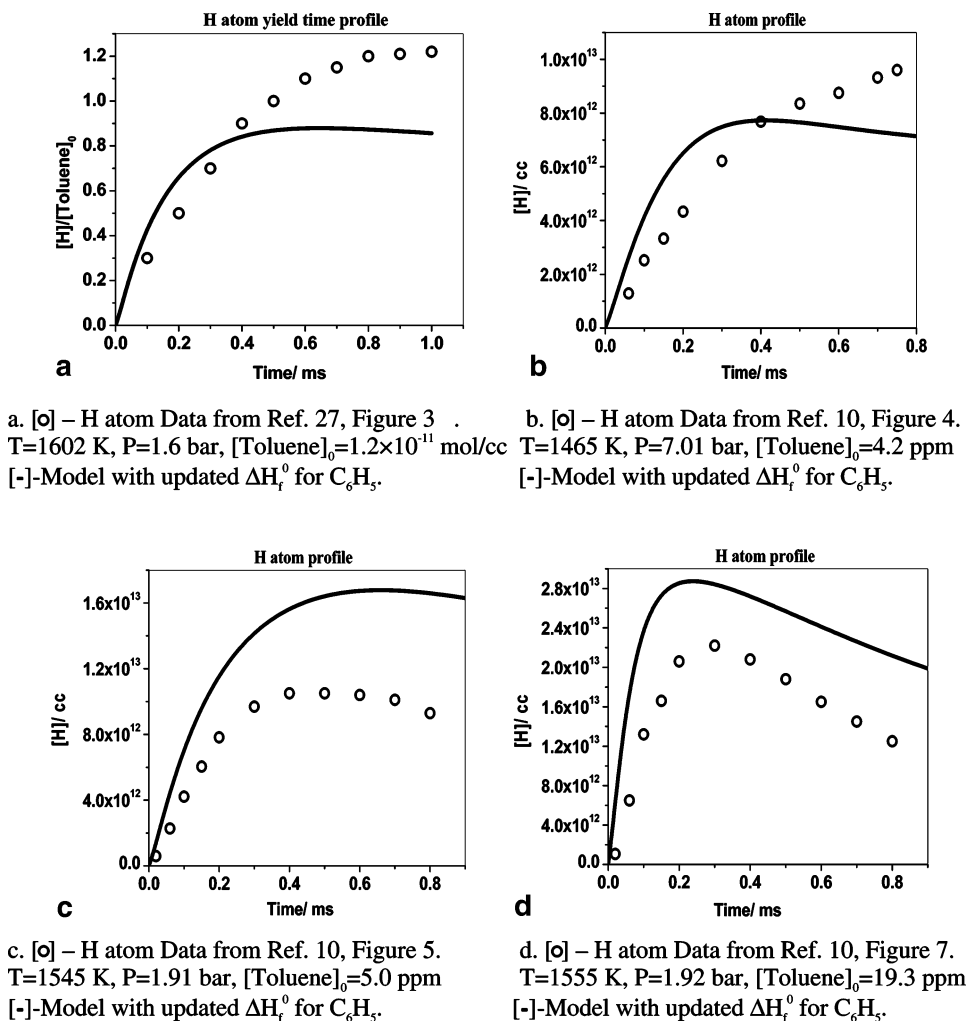
a. [o] – H atom Data from Ref. 27, Figure 3 .
T=1602 K, P=1.6 bar, [Toluene]$_0$=1.2×10^{-11} mol/cc
[-]-Model with updated ΔH_f^0 for C_6H_5.

b. [o] – H atom Data from Ref. 10, Figure 4.
T=1465 K, P=7.01 bar, [Toluene]$_0$=4.2 ppm
[-]-Model with updated ΔH_f^0 for C_6H_5.

c. [o] – H atom Data from Ref. 10, Figure 5.
T=1545 K, P=1.91 bar, [Toluene]$_0$=5.0 ppm
[-]-Model with updated ΔH_f^0 for C_6H_5.

d. [o] – H atom Data from Ref. 10, Figure 7.
T=1555 K, P=1.92 bar, [Toluene]$_0$=19.3 ppm
[-]-Model with updated ΔH_f^0 for C_6H_5.

Figure 10. H atom profiles from shock tube−ARAS experiments.
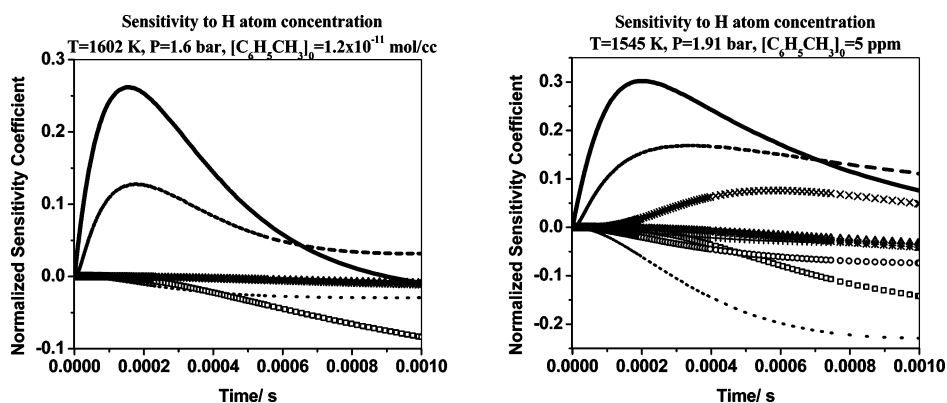
Figure 11. Sensitivity analyses. [—] − $H + C_6H_5CH_2 = C_6H_5CH_3$, [---] − $CH_3 + C_6H_5 = C_6H_5CH_3$, [···] − $C_6H_5CH_3 + H = C_6H_5CH_2 + H_2$, [+] − $C_6H_5CH_3 + H = C_6H_6 + CH_3$, [*] − $H_2CCCH + H = AC_3H_4$, [□] − $H_2CCCH + H = C_3H_2 + H_2$, [△] − $CH_3 + H(+M) = CH_4(+M)$, [○] − $C_6H_6 = C_6H_5 + H$, [×] − $C_6H_5CH_2 = C_5H_5 + C_2H_2$.

and have from their high-temperature measurements of the rate of dissociation via reaction −1b and the forward association rate measured by Ackermann et al.[45] derived the heat of formation for the benzyl radical to be 51.6 ± 1 kcal/mol.[28] On the basis of detailed modeling they have concluded that a value of 51.5 kcal/mol best fits their experimental data. This number would appear at first view to be an outlier with respect to the other experimental measurements that have been reported in the review. However one should note that this number overlaps the Hippler and Troe[46] recommended value of 50.3 ± 1 kcal/mol, which represents the largest experimental value in the

IUPAC review[35] and the more recent recommended value by Song et al.[47] of 50.2 ± 2 kcal/mol based on high-temperature decomposition experiments on benzylamine. The three other experimental measurements used in the review have used experimental heats of reaction to derive the heat of formation for the benzyl radical. Tsang and Walker[48] used the heat of the reaction at 1100 K derived for *n*-pentylbenzene → benzyl + *n*-C_4H_9 to obtain the heat of formation for benzyl while Elmaimouni et al.[49] used the heat of reaction for $C_6H_5CH_2 + O_2 = C_6H_5CH_2OO$ to derive ΔH_f^0 for benzyl based on an estimated enthalpy of formation of 29 kcal/mol for $C_6H_5CH_2$-

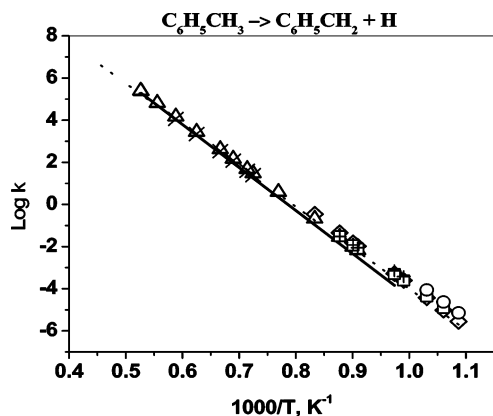**C$_6$H$_5$CH$_3$ -> C$_6$H$_5$CH$_2$ + H**

Figure 12. (-) Derived rate coefficients from current work (1027–1897 K); (•••) Baulch et al.[29] (920–2200 K); (X) Braun-Unkhoff et al.[10] (1380–1700 K); (□) Price[31] (943–1140 K); (○) Brooks et al.[53] (920–970 K); (◇) Brand et al.[54] (300–1200 K, plotted over *T* range 920–1200 K); (+) Szwarc[4] (1010–1140 K); (△) Hippler et al.[13] (1100–1900 K).

OO. The Ellison et al.[50] recommendation for the benzyl heat of formation was derived from the equilibrium constant for $C_6H_5CH_3 + CH_3O^- \rightarrow C_6H_5CH_2^- + CH_3OH$ and gas-phase acidities for toluene and methanol. Among these experimental recommendations the Braun-Unkhoff et al.[28] value appears to be the one with the least uncertainty simply because of the well characterized forward and reverse rate coefficients for channel 1B and the well-known thermochemistry for the other species in the reaction, viz. toluene and the H atom. The recommenda-

tions of two recent theoretical computations by Henry et al.[51] and Janoschek and Rossi[52] also fall within the error bars of the Braun-Unkhoff et al.[28] value. Consequently we have chosen to use the recommendation of Braun-Unkhoff et al.[28] of 51.5 kcal/mol for $\Delta H_f^0{}_{298K}$ of $C_6H_5CH_2$. With this updated value for the heat of formation for benzyl the derived reverse rate parameters for channel 1B are shown in Table 4. The derived rate constants

TABLE 4

reaction	A	n	E_a
H + C$_6$H$_5$CH$_2$ → C$_6$H$_5$CH$_3$	5.384×10^{13}	0.11305	0 (fit to HK rate 1027 K < T < 1897 K)
reverse	1.524×10^{16}	−0.04	93 499 ($\Delta H_f^0{}_{298K}$ from Braun-Unkhoff et al.)

for the reverse reaction (reaction −1b) using the updated heat of formation for benzyl are approximately a factor of 2.3–1.9 lower than the rate constants derived using the IUPAC recommended $\Delta H_f^0{}_{298K}$ and in line with other literature rate coefficients. Figure 12 shows a compilation at high temperatures of the current rate constants derived for reaction −1b plotted along with other literature recommendations. The current derived rate constants fall within 30%-10% of the latest Baulch et al.[29] recommendations over the temperature range 1200−1800 K for −1b with the larger deviations at lower temperatures. The excellent fit offers additional support for the $\Delta H_f^0{}_{298K}$ for $C_6H_5CH_2$ used in the current work. Branching ratios for the two primary steps in toluene dissociation vary from 0.39 to 0.52 over the temperature range 1200−1800 K compared to the initial calculations of 0.04 to 0.1 with the original heats of formation.
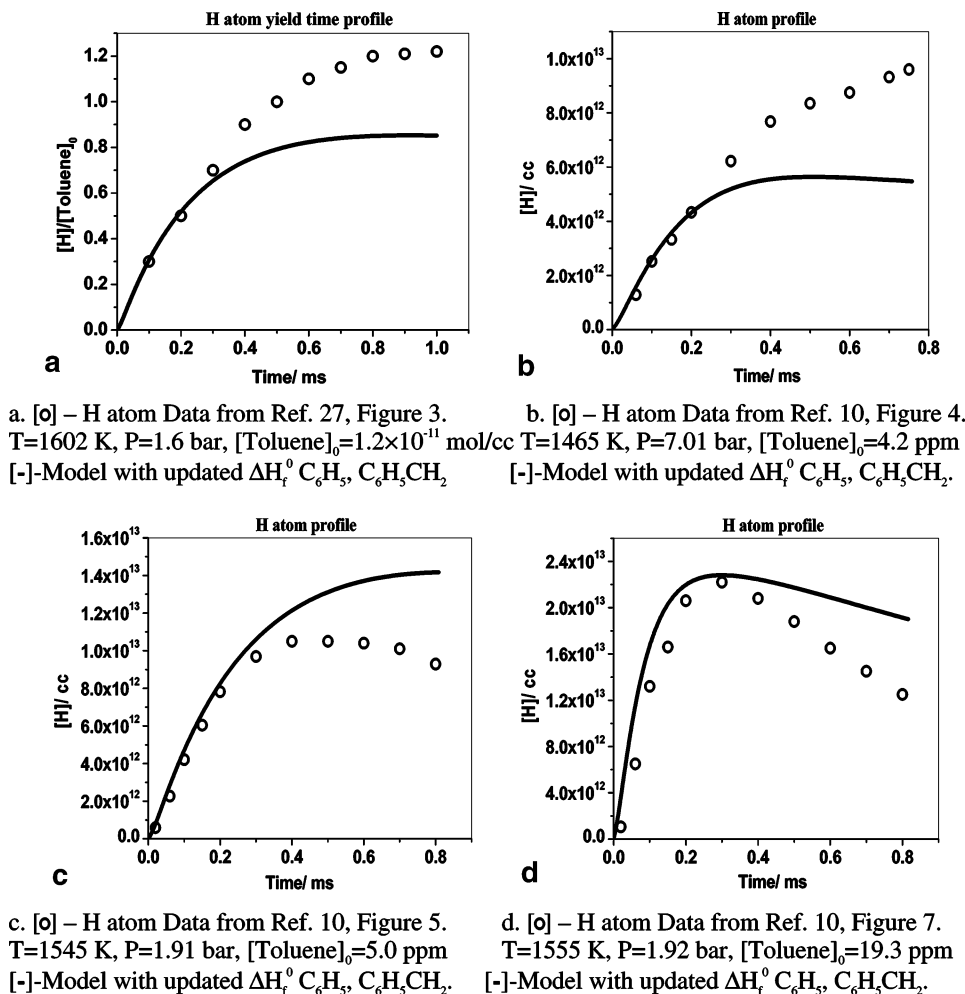

a. [○] – H atom Data from Ref. 27, Figure 3.
T=1602 K, P=1.6 bar, [Toluene]$_0$=1.2×10^{-11} mol/cc
[-]-Model with updated ΔH_f^0 C$_6$H$_5$, C$_6$H$_5$CH$_2$

b. [○] – H atom Data from Ref. 10, Figure 4.
T=1465 K, P=7.01 bar, [Toluene]$_0$=4.2 ppm
[-]-Model with updated ΔH_f^0 C$_6$H$_5$, C$_6$H$_5$CH$_2$.

c. [○] – H atom Data from Ref. 10, Figure 5.
T=1545 K, P=1.91 bar, [Toluene]$_0$=5.0 ppm
[-]-Model with updated ΔH_f^0 C$_6$H$_5$, C$_6$H$_5$CH$_2$.

d. [○] – H atom Data from Ref. 10, Figure 7.
T=1555 K, P=1.92 bar, [Toluene]$_0$=19.3 ppm
[-]-Model with updated ΔH_f^0 C$_6$H$_5$, C$_6$H$_5$CH$_2$.

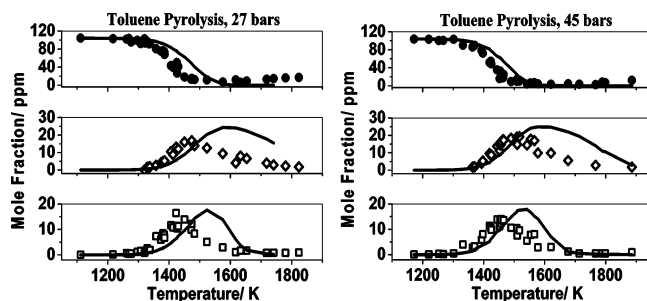**Figure 13.** H atom profiles from shock tube−ARAS experiments.

Figure 14. HPST profiles: (●) $C_6H_5CH_3$; (□) C_6H_6; (◇) CH_4; (-) detailed model with updated $\Delta H_f{}^0$ for C_6H_5 and $C_6H_5CH_2$.

We have also fit the rate constants for reactions −1a and −1b to a standard Arrhenius form using the updated thermochemical information for the phenyl and benzyl radicals. The fits translate to the rate parameters given in Table 5. The

TABLE 5

reaction	A	E_a
$C_6H_5CH_3 \rightarrow CH_3 + C_6H_5$	4.068×10^{16}	97647 (fit to HK rate 1027 K < T < 1897 K)
$C_6H_5Ch_3 \rightarrow H + C_6H_5CH_2$	1.113×10^{16}	93396 (fit to KH rate 1027 K < T < 1897 K)

difference in the activation energies can be understood in terms of the heats of reaction for −1a and −1b. With the updated heats of formation at 298 K for phenyl (78.6 kcal/mol) and benzyl (51.5 kcal/mol) derived from the current experiments and modeling and the known heats of formation for toluene (12.0 kcal/mol), H atom (52.1 kcal/mol) and CH_3 (35.0 kcal/mol), the heats of reaction (ΔH_r) at 298 K translate to 101.6 kcal/mol for reaction −1a and 91.6 kcal/mol for reaction −1b. This difference in the ΔH_r can be seen in the higher E_a for −1a. Furthermore, the larger A factor for −1a can be attributed to the formation of two radical species in contrast to the formation of an atom and a radical in reaction −1b.

With the updated forward and reverse rate coefficients for channels 1A and 1B, we have modeled the H atom profile experiments in Figure 6a−d as well as our own single pulse shock tube profiles. Figures 13a−d and 14 depict the fits to the H atom data as well as single pulse shock tube profiles, respectively. The change in benzyl heat of formation alters significantly the fits to the H atom temporal profiles that were obtained with the updated $\Delta H_f{}^0$ for C_6H_5. With the updated $\Delta H_f{}^0$ for C_6H_5 and $C_6H_5CH_2$ the model is able to capture the experimental trends over a wide range of conditions, specifically at short times <300 μs when the only sensitive reactions are the two primary channels. The model does not lose its predictive capability for the single pulse shock tube profiles with a good fit to the $C_6H_5CH_3$, CH_4, and C_6H_6 profiles. The fits to CH_4 profiles coupled with the H atom fits validate the high-pressure limiting rate coefficients and branching ratios extracted for the two primary channels 1A and 1B.

Conclusions

The pyrolysis of toluene has been studied at reflected shock pressures of 27 and 45 bar in the single pulse shock tube over the temperature range 1200−1900 K. Species profiles were obtained for a number of the smaller hydrocarbons and single ring aromatic species. Total rate coefficients for the decay of toluene as well as formation rate coefficients for C_6H_6, CH_4, C_2H_2 and C_4H_2 were derived using the experimental data. A detailed model consisting of 262 reactions and 87 species was assembled to describe the decay of toluene as well as the

formation of the observed intermediates. The primary dissociation channels in toluene represent the most dominant and sensitive reactions in this system and consequently utilizing recent theoretical predictions of the association rate coefficients in combination with revised heats of formation for $C_6H_5CH_2$ (51.5 ± 1.0 kcal/mol) and the C_6H_5 radicals (78.6 ± 1.0 kcal/mol) we have successfully modeled H atom profiles from prior experimental studies in combination with toluene, CH_4 and C_6H_6 profiles in our current single pulse experiments thereby lending credibility to the high-pressure rate constants ($k_{-1a,\infty} = (4.62 \times 10^{25})T^{-2.53}\exp[-104.5 \times 10^3/RT]$ s^{-1} and $k_{-1b,\infty} = (1.524 \times 10^{16})T^{-0.04}\exp[-93.5 \times 10^3/RT]$ s^{-1}) and branching ratios that have been derived for these primary dissociation steps.

Supporting Information Available: Tables ST1a and ST1b, listing experimental data from the single pulse shock tube (species mole fractions and reaction conditions) and Table ST2, listing the detailed toluene pyrolysis model developed as part of this work. This material is available free of charge via the Internet at http://pubs.acs.org.

References and Notes

(1) Manion, J. A. Combustion Kinetics Databases for Real Fuels. Presented at the International Workshop on CHEMKIN in Combustion, Chicago, IL, July 25, 2004.

(2) Farrell, J. T. *Fuels Workshop*; NIST: Gaithersburg, MD, 2003.

(3) Pope, C. A., III; Burnett, T. R.; Thurston, D. G.; Thun, J. M.; Calle, E.; Krewski, D.; Ito, K. *J. Am. Med. Assoc.* **2002**, *287*, 1132−1141.

(4) Szwarc, M. *J. Chem. Phys.* **1948**, *16*, 128−136.

(5) Szwarc, M. *Chem. Rev.* **1950**, *47*, 75−173.

(6) Smith, R. D. *Combust. Flame* **1979**, *35*, 179.

(7) Smith, R. D. *J. Phys. Chem.* **1979**, *83*, 1553−1563.

(8) Astholz, D. C.; Durant, J.; Troe, J. *Proc. Comb. Inst.* **1980**, *18*, 885.

(9) Pamidimukkala, K. M.; Kern, R. D.; Patel, M. R.; Wei H. C.; Kiefer, J. H. *J. Phys. Chem.* **1987**, *91*, 2148−2154.

(10) Braun-Unkhoff, M.; Frank, P.; Just, T. H. *Proc. Comb. Inst.* **1988**, *22*, 1053−1061.

(11) Brouwer, L. D.; Muller-Markgraf, W.; Troe, J. *J. Phys. Chem.* **1988**, *92*, 4905.

(12) Rao, V. S.; Skinner, G. B. *J. Phys. Chem.* **1989**, *93*, 1864.

(13) Hippler, H.; Reihs, C.; Troe, J. *Z. Phys. Chem., Neue Folge* **1990**, *167*, 1−16.

(14) Colket, M. B.; Seery, D. J. *Proc. Comb. Inst.* **1994**, *25*, 883−891.

(15) Kern, R. D.; Chen, H.; Singh, H. J.; Xie, K.; Kiefer, J. H.; Sidhu, S. S. Turbulence and Molecular Processes in Combustion. In *Proceedings of the Sixth Toyota Conference*; Takeno, T., Ed.; Elsevier: The Netherlands, 1992; 117−133.

(16) Lindstedt, R. P.; Maurice, L. Q. *Combust. Sci. Technol.* **1996**, *120*, 119−167.

(17) Sivaramakrishnan, R.; Tranter, R. S.; Brezinsky, K. *Combust. Flame*, **2004**, *139*, 340−350.

(18) Sivaramakrishnan, R.; Tranter, R. S.; Brezinsky, K. *Proc. Combust. Inst.* **2005**, *30*, 1165−1173.

(19) Sivaramakrishnan, R.; Tranter, R. S.; Brezinsky, K. *J. Phys. Chem. A* **2006**. In press.

(20) Tranter, R. S.; Fulle, D.; Brezinsky, K. *Rev. Sci. Instrum.* **2001**, *72*, 3046−3054.

(21) Tranter, R. S.; Sivaramakrishnan, R.; Srinivasan, N.; Brezinsky, K. *Int. J. Chem. Kinet.* **2001**, *33*, 722−731.

(22) Tranter, R. S.; Sivaramakrishnan, R.; Allendorf, M. D.; Brezinsky, K. *Phys. Chem. Chem. Phys.* **2002**, *4*, 2001−2010.

(23) NIST Chemical Kinetics Database on the Web, Standard Reference Database 17, Version 7.0 (Web Version), Release 1.3. http://kinetics.nist.gov.

(24) Astholz, D. C.; Troe, J. *J. Chem. Soc., Faraday Trans. 2* **1982**, *78*, 1413−1421.

(25) Banerjee, D. K.; Matei, V.; Vantu, V. *Rev. Roum. Chim.* **1982**, *27*, 621−628.

(26) Bruinsma, O. L. S.; Geertsman, R. S.; Bank, P.; Moulijn, J. A. *Fuel* **1988**, *67*, 327−333.

(27) Eng, R. A.; Gebert, A.; Goos, E.; Hippler, H.; Kachiani, C. *Phys. Chem. Chem. Phys.* **2002**, *4*, 3989−3996.

(28) Braun-Unkhoff, M.; Frank, P.; Just, T. H. *Ber. Bunsen-Ges. Phys. Chem.* **1990**, *94*, 1417−1425.

(29) Baulch, D. L.; Bowman, C. T.; Cobos, C. J.; Cox, R. A.; Just, T. H.; Kerr, J. A.; Pilling, M. J.; Stocker, D.; Troe, J.; Tsang, W.; Walker, R. W.; Warnatz, J. *J. Phys. Chem. Ref. Data* **2005**, *34*, 757−1397.

(30) Lifshitz, A. In *Handbook of Shock Waves*; Ben-Dor, G., Igra, O., Elperin, T., Eds.; Academic Press: San Diego, CA, 2001; Vol. 3.

(31) Price, S. J. *Can. J. Chem.* **1962**, *40*, 1310−1317.

(32) (a) Klippenstein, S. J.; Harding, L. B.; Georgievskii, Y. Submitted to *Proc. Combust. Inst.* 2006. (b) Harding, L. B. Personal communication.

(33) Emdee, J. L.; Brezinsky, K.; Glassman, I. *J. Phys. Chem.* **1992**, *96*, 2151−2161.

(34) Klotz, S. D.; Brezinsky, K.; Glassman, I. *Proc. Combust. Inst.* **1998**, *27*, 337−344.

(35) Ruscic, B.; Boggs, J. E.; Burcat, A.; Csaszar, A. G.; Demaison, J.; Janoschek, R.; Martin, J. M. L.; Morton, M.; Rossi, M. J.; Stanton, J. F.; Szalay, P. G.; Westmoreland, P. R.; Zabel, F.; Berces, T. *J. Phys. Chem. Ref. Data* **2005**, *34*, 573−656.

(36) Burcat, A.; Ruscic, B. Ideal Gas Thermochemical Database with updates from Active Thermochemical Tables: ftp://ftp.technion.ac.il/pub/supported/aetdd/thermodynamics; 16 Sep 2005. Mirrored at http://garfield-.chem.elte.hu/Burcat/burcat.html; 16 Sep 2005.

(37) Davico, G. E.; Bierbaum, V. M.; DePuy, C. H.; Ellison, G. B.; Squires, R. R. *J. Am. Chem. Soc.* **1995**, *117*, 2590−2599.

(38) Rolland, S.; Simmie, J. M. *Int. J. Chem. Kinet.* **2005**, *37* (3), 119−125. Downloaded from http://www.nuigalway.ie/chem/combust.htm#downloads.

(39) Kee, R. J.; Rupley, F. M.; Miller, J. A.; Coltrin, M. E.; Grcar, J. F.; Meeks, E.; Moffat, H. K.; Lutz, A. E.; Dixon-Lewis, G.; Smooke, M. D.; Warnatz, J.; Evans, G. H.; Larson, R. S.; Mitchell, R. E.; Petzold, L. R.; Reynolds, W. C.; Caracotsios, M.; Stewart, W. E.; Glarborg, P.; Wang, C.; Adignun, O. *CHEMKIN Collection, Release 3.6 ed.*, Reaction Design Inc.: San Diego, CA, 2000.

(40) Robaugh, D.; Tsang, W. *J. Phys. Chem.* **1986**, *90*, 4159−4163.

(41) Price, S. J. W.; Trotman-Dickenson, A. F. *J. Chem. Soc.* **1958**, 4205−4207.

(42) Horn, C.; Frank, P.; Tranter, R. S.; Schaugg, J.; Grotheer, H.; Just, T. H. *Proc. Combust. Inst.* **1996**, *26*, 575−582.

(43) McMillen, D. F.; Golden, D. M. *Annu. Rev. Phys. Chem.* **1982**, *33*, 493−532.

(44) Kiefer, J. H.; Mizerka, L. J.; Patel, M. R.; Wei, H.-C. *J. Phys. Chem.* **1985**, *89*, 2013−2019.

(45) Ackermann, L.; Hippler, H.; Pagsberg, P.; Reihs, C.; Troe, J. *J. Phys. Chem.* **1990**, *94*, 5247−5251.

(46) Hippler, H.; Troe, J. *J. Phys. Chem.* **1990**, *94*, 3803−3806.

(47) Song, S.; Golden, D. M.; Hanson, R. K.; Bowman, C. T. *J. Phys. Chem. A* **2002**, *106*, 6094−6098.

(48) Walker, J. A.; Tsang, W. *J. Phys. Chem.* **1990**, *94*, 3324−3327.

(49) Elmaimouni, L.; Minetti, R.; Sawerysyn, J. P.; Devolder, P. *Int. J. Chem. Kinet.* **1993**, *25*, 399.

(50) Ellison, G. B.; Davico, G. E.; Bierbaum, V. M.; DePuy, C. H. *Int. J. Mass. Spectrom. Ion Proc.* **1996**, *156*, 109−131.

(51) Henry, J.; Parkinson, C. J.; Mayer, P. M.; Radom, L. *J. Phys. Chem. A* **2001**, *105*, 6750−6756.

(52) Janoschek, R.; Rossi, M. J. *Int. J. Chem. Kinet.* **2002**, *34*, 550−560.

(53) Brooks, C. T.; Cummins, C. P. R.; Peacock, S. J. *Trans. Faraday. Soc.* **1971**, 67.

(54) Brand, U.; Hippler, H.; Lindemann, L.; Troe, J. *J. Phys. Chem.* **1990**, *94*, 6305−6316.